Colloid and Interface Science Communications 16 (2017) 14–18

Contents lists available at ScienceDirect

Colloid and Interface Science Communications

journal homepage: www.elsevier.com/locate/colcom

Rapid Communication

Synthesis and Assembly of Gold and Iron Oxide Particles Within an Emulsion Droplet; Facile Production of Core@Shell Particles

Suchanuch Sachdev [a], Rhushabh Maugi [a], Caroline Kirk [a], Zhaoxia Zhou [b], Steven D.R. Christie [a], Mark Platt [a,*]

[a] Department of Chemistry, Loughborough University, Loughborough LE11 3TU, United Kingdom
[b] Department of Materials, Loughborough University, Loughborough LE11 3TU, United Kingdom

ARTICLE INFO

Article history:
Received 15 August 2016
Received in revised form 2 December 2016
Accepted 14 December 2016
Available online xxxx

Keywords:
Microfluidic
Emulsion
Liquid-liquid
Pickering emulsion
Core@shell

ABSTRACT

Here we report a method for synthesising and assembling nanomaterials at the liquid-liquid interface of an emulsion droplet, resulting in a simple strategy for producing hollow Au shells, or Fe_3O_4@Au core@shell particles. Mercaptododecanoic acid stabilised Au nanoparticles were added to the aqueous continuous phase, in order to stabilise hexane emulsion droplets formed within a microfluidic chip. The diameters of Au Pickering emulsions could be controlled by varying the flow rates, this produce hollow particles. The addition of a second nanoparticle, Fe_3O_4 (average diameter of 12 nm), into the organic phase produced core@shell particles. The diameter of the resultant material was determined by the concentration of the Fe_3O_4. This report is the first to demonstrate Pickering emulsions within a microfluidics chip for the production of Fe_3O_4@Au particles, and it is believed that this could be a versatile platform for the large scale production of core@shell particles.

Synthesis and fabrication methods for nanoparticles have evolved to the extent that particle size, shape, and composition can be controlled. As such they have been integrated into many aspects of modern life [1]. Gold nanoparticles, Au-NPs, of various morphologies are commonly found as they have numerous applications in catalysis [2], biosensing [3] and therapeutics [4]. Anisotropic particles, in particular gold nanosheets and core@shell particles have gained particular attention [5]. They possess enhanced optical properties for the treatment of tumours [6], enhanced Raman detection [7] and optical sensors [8]. As a result several chemical synthesis strategies have been developed for single and two phase systems [9]. However, most synthesises strategies that lead to high anisotropy require organic solvents, high temperatures, hard reducing agents, polymer and molecular capping agents, although alternative "green" chemistries are emerging [4,6,10].

Conversely, electrochemical techniques allow a degree of control over the growth and assembly of the material through the applied potential or template, allowing nanomaterials to be formed at the solid-liquid and liquid-liquid (liq-liq) interface [11,12]. The interface between two immiscible liquids offers a defect free, reproducible substrate to grow metals. This allows the material to be easily recovered, as the majority of the formed particles remain at the interface upon creation [13]. The interface between two liquids can also be used to assemble nanoparticles with their spacing and composition at the interface as shown in Fig. 1, controlled via capping ligands [8]. The assembly of nanomaterials at the liq-liq interface is spontaneous due to the favourable stabilisation of the interfacial free energy and was first discovered by Ramsden [14] and Pickering [15]. The preferred location at the interface is determined by the Young's equation and by tailoring the surface chemistry of the particles. The contact angle of the particle at the interface can be controlled and can be used to create oil-in-water or water-in-oil emulsions, known generally as Pickering Emulsions. Pickering emulsion synthesis strategies have assembled a range of both polymer and inorganic materials at the interface of the droplets [16–19], and when materials are present in both phases even core@shell particles can be synthesised [20]as shown in Fig. 1 iii.

In this paper we present a strategy for producing Fe_3O_4@Au particles using Pickering emulsions. The combination of a magnetic core and a biocompatible, chemically inert, and easily functionalized shell, offer biomedical, separation or analytical applications. Au shells have been used as localised hyperthermia treatments of cancer [6], and Iron oxide superparamagnetic materials have been used as contrast agents for MRI imaging [21]. We present the first demonstration of Pickering emulsions within a microfluidics chip for the production of Fe_3O_4@Au particles, where the core diameter can be controlled by the concentration of NP1 in the organic phase as shown in Fig. 1 ii. The technique has the advantages of not requiring long reaction times, surfactants or templates to produce the asymmetric materials.

1. Chemicals and reagents

The following chemicals are from Sigma Aldrich, U.K. and unless stated the chemicals were used without purification. Sodium Dodecyl Sulfate (SDS) (436143), Iron (ll) chloride tetrahydrate ($FeCl_2 \cdot 4H_2O$)

* Corresponding author.
E-mail address: m.platt@lboro.ac.uk (M. Platt).

http://dx.doi.org/10.1016/j.colcom.2016.12.005

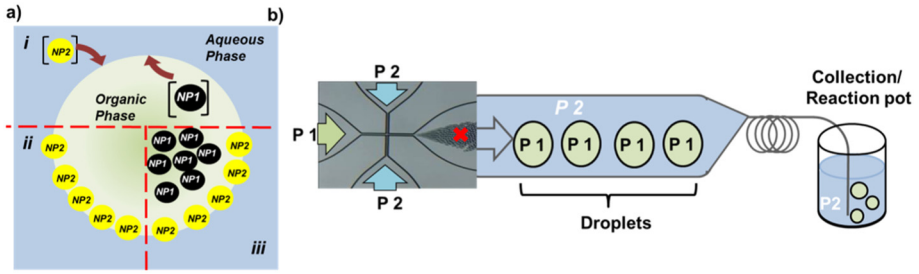

Fig. 1. a) Schematic of liquid-liquid interface with nanoparticles NP1 and NP2 presynthesised and dispersed in the organic of aqueous phase respectively. ii. Particle at a Pickering emulsion interface. iii. Core@shell Pickering emulsion. b). Schematic of the fluidic assembly and droplet collection. P1, P2 represents the organic and aqueous phase respectively. The droplets flowed through a tube 5 cm long into a collection vial.

(220299), Iron (lll) chloride hexahydrate ($FeCl_3 \cdot 6H_2O$) (236489), ammonium hydroxide ($NH_3 \cdot H_2O$) (338818), Oleic acid (364525), perchloric acid (244252), Gold (lll) chloride trihydrate (≥49%) (G4022-1G), Tetraoctylammonium bromide (98%) (294136), 12-mercaptododecanoic acid (12-MDA) (675067), sodium borohydride (98%) (452882). The following chemicals are from VWR chemicals, U.K. and unless stated the chemicals were used without purification. Hexane (24,580.324), ethanol absolute (20,821.330), toluene (28,676.322), were used. Deionized (DI) water was collected from Millipore water purification system having 18 Ω cm conductance) was used throughout.

Microfluidics instruments were supplied by Dolomite, A 14 μm etch depth Dolomite hydrophilic x-junction "small droplet chip" (Part No. 3200136), Dolomite Mitos P-Pump basic (Part No. 3200175) were controlled via the Dolomite Mitos Flow Control Centre Version 2.2.15

Synthesis of hydrophobic nanomagnetic particles (250 mL) scale. $FeCl_{12} \cdot 4H_2O$ (12 g) and $FeCl_3 \cdot 6H_2O$ (24.5 g) were dissolved in DI-water (62.5 mL) in a 250 mL three neck bottle. The flask was placed in an ice bath. $NH_3 \cdot H_2O$ (50 mL) was added rapidly with vigorous stirring. The flask was left in the ice bath for 45 min. The solution was rapidly heated to 85 °C for 1 h. Oleic acid (7.5 mL) was then added and the solution was further heated for another 1 h. The flask was cooled to room temperature and the slur was transferred to a 150 mL beaker. Slur was washed 3 times with ethanol (50 mL) and each time the black magnetite was collected using a block magnet. The slur was then washed 3 times with DI-water (50 mL) before being washed 3 times with 20% perchloric acid (50 mL) to dissolve $Fe(OH)_2$ and $Fe(OH)_3$. The slur was again washed 3 times with DI-water (50 mL), before being washed three times with ethanol (50 mL). Hexane (87.5 mL) was added to the resultant particles so to disperse well, this was called ferrofluid. The particle concentration was determined by weighing the mass of material that remained after the evaporation of a known volume of solvent.

Synthesis of gold nanoparticles coated with 12-mercaptododecanoic acid in toluene. Gold nanoparticles were prepared by the previously reported technique [22], briefly $HAuCl_4$ (0.05 M, 4 mL) was mixed with 11 mL of 0.05 M tetraoctylammonium bromide in toluene (0.05 M, 11 mL) in a vial. The mixture was left stirring for a minimum of 2 h, the organic phase was then transferred to another vial and 12-mercaptododecanoic acid (1200 μL) was added to it followed by freshly prepared $NaBH_4$ (0.4 M, 25 mL) with vigorous stirring. Colour change from orange to deep brown indicates completion of the reaction. The mixture was left stirring for a minimum of 3 h. The organic phase was separated from the mixture and transferred to a clean vial. The organic phase (500 μL) of the Au-NP solution was transferred to an Eppendorf tube allowing the solvent to be evaporated to dryness. Ethanol (1500 μL) was then added to the precipitate, followed by 2 drops of NaOH (5 M). The Eppendorf tube was vortexed to disperse the pellet and then kept in the freezer for 16 h following a centrifuged process at 12000 rpm for 5 min. The supernatant was removed and washed twice with ethanol (1000 μL) followed by DI-water (100 μL). At this point the particles had dispersed into the aqueous solution and it appeared brown.

Creation of emulsion droplets, hexane, (P1) and aqueous solution (P2) were connected to the droplet chip as guided by the manufacturer instructions. P2 was the continuous phase and the droplets size of P1 was controlled by varying the flow rates of P1:P2. The droplet size was observed through a Celestron LCD digital microscope Model ~44,340. Moreover, the droplet size was determined by analysing an image taken on the microscope and was measured by a point marked X as shown in Fig. 1b. The droplet was collected for 2 h and left for evaporation for 2–3 h.

Collection of particles, the collected sample was centrifuged (12,000 rpm, 5 mins) then the supernatant was discarded and replaced with acetonitrile (500 μL). The washing process was repeated with DI-water. The sample was then re-dispersed in DI-water (500 μL). When the sample contained iron oxide nanoparticles, the solution is purify by placing on a magrack (GE, healthcare, UK) for 2 min. The supernatant was discarded and replaced with DI-water (100 μL) then it was placed on a sonication bath for 1 min. The washing process was repeated three times with DI-water and twice with acetonitrile. The sample was then re-dispersed in either water or acetone (100 μL).

Scanning electron microscopy (SEM) samples were prepared by dropping the suspension onto conductive copper pad. The SEM used for imaging was a table top SEM Hitachi TM3030, an FEG-SEM JEOL 7800F, a Leo (Zeiss) 1530-VP FEG-SEM.

Transmission electron microscopy (TEM) specimens were prepared by ultrasonicating the suspensions followed by pipetting onto standard holey carbon support TEM grids. A Jeol 2000FX TEM equipped with an Oxford Instruments (INCA350) energy dispersive X-ray spectroscopy (EDS) system was used to characterise the samples. The TEM was operated with 200 kV accelerating voltage in conventional bright field mode. Selected area electron diffraction (SAED) patterns were recorded to identify the crystallinity of the particles.

The magnetic properties of the beads were measured with a superconducting quantuminterference device (SQUID) magnetometer (Quantum Design, San Diego, CA, USA) at room temperature as described previously [23].

Samples were prepared for analysis by Powder X ray Diffraction (PXRD) from suspensions. The suspensions were dropped onto silicon substrates and the liquid allowed to evaporate before being placed into Perspex sample holders. The sample holders were loaded onto a Bruker D8 Advance Powder X ray Diffractometer set up in reflection geometry with Cu $K\alpha_1$ radiation (1.54056 Å), selected from a Ge 111 monochromator and a LYNXEYE™ 1D detector. Data were collected over the 2θ range 30–80° 2θ with a step size of 0.007° and a count time of 2 s per step.

We have previously shown the emulsion templated self-assembly of iron oxide nanoparticles using oil-in-water emulsions. By changing the nanoparticle concentration, NP1, shown in Fig. 1a, the resulting microparticles diameter can be controlled, creating a high through put

Table 1
Parameters for experiments using Pickering emulsions (A1–3), and the synthesis of particles at the liquid-liquid interface (B1, 2). P1, P2 is the organic phase, and aqueous phase respectively.

Experiment	Classification	P1 (hexanes)	P2 (aqueous)
A1	Fe_3O_4 CORE	3 mg/mL ferrofluid	2% (wt/wt) SDS
A2	Pickering emulsion (Au SHELL)	–	5 mg/mL MDA-Au particles
A3	Fe_3O_4@Au (CORE@SHELL)	3 mg/mL ferrofluid	5 mg/mL MDA-Au particles

synthesis of uniform Fe_3O_4 micro-particles [24]. Here we use a similar setup within the microfluidic chip, listed as experiment A1 in Table 1. Oleic acid stabilised Fe_3O_4 particles are suspended into P1 at 3 mg/mL, TEM and SQUID data for the feedstock ferrofluid is given in Figs. S1 and 2 respectively. The flow rates of P1 and P2 were adjusted to give emulsion droplets, stabilised by SDS, with an average size of 11 μm ± 1.54, which are then collected in an open vial allowing the hexane to evaporate. The resultant microparticles of Fe_3O_4 had a mean diameter of 1.4 μm ± 0.05, shown in Fig. 2a. By varying the concentration of Fe_3O_4, or the droplet size, the resultant microparticle diameter can be varied [24].

To form an AuNP shell on the outside of the iron oxide, 12-mercaptododecanoic acid, 12-MDA, stabilised particles were synthesised as described above. Typical TEM bright field image and diffraction pattern are shown in Fig. S3 which illustrate their crystal size between (100–400 nm) and amorphous nature. These particles are known to sit at the toluene-water interface [25]. Absorbance spectra for the particle are shown in Fig. 2b. To test the ability of these particles to stabilise droplets, the AuNPs were added to P2 at 5 mg/mL, in the absence of any Fe_3O_4 within P1, the flow rates of P1 and P2 adjusted to give emulsion droplets of 7.7 μm ± 0.73, experiment A2 in Table 1. It is important to note that in this configuration no SDS or other surfactants are present, and that the droplets formed at the junction are stabilised by the AuNPs themselves. In the control experiment, where no SDS or AuNPs are present, no droplets was formed and a jetting regime is maintained across all P1:P2 flow ratios.

Forming droplets demonstrates that the AuNPs are surface active and that their absorbance onto the interface is rapid. The resultant emulsion droplets were then collected allowing hexane to evaporate, before imaging. SEM of AuNP shells are shown in Fig. 2c (EDS analysis shown in supplementary Fig. S2). The average particle size obtained was 2.3 μm ± 0.56 Given the droplets were initially 7.7 μm ± 0.73 in size, it demonstrates that the size of initial droplets created in the fluidic device are not maintained. This may be due to either the surface coverage of the AuNPs on the droplets surface, being <1, and that the hexane is evaporating quicker than the AuNPs can form a full shell. More likely given the stabilising ligand (12-MDA), maybe a contributing factor and AuNP being transfer into the hexane layer as the droplet shrinks.

Analysis of the Pickering emulsion shells using TEM, Fig. 2d, shows particles of differing morphologies under the electron beam. Smaller particles seemed to be more stable and maintained their spherical shape during observation, whist larger particles, insert Fig. 2d, collapsed under the electron beam. This indicates that particles are not stable under the 200 kV beam used in TEM, analysis of particles using SEM with an operating voltage not >20 kV does not cause the particles to change. The stability of the hollow particles in biological solutions, or under applied forces still needs to be investigated. The different sizes of particles are then thought to be the result of this internalisation process at different stages.

For experiment A3 as shown in Table 1, the core and shell concepts, demonstrated in A1 and A2 were combined together, and shown schematically in Fig. 1aiii, to create an iron oxide core and AuNP Pickering

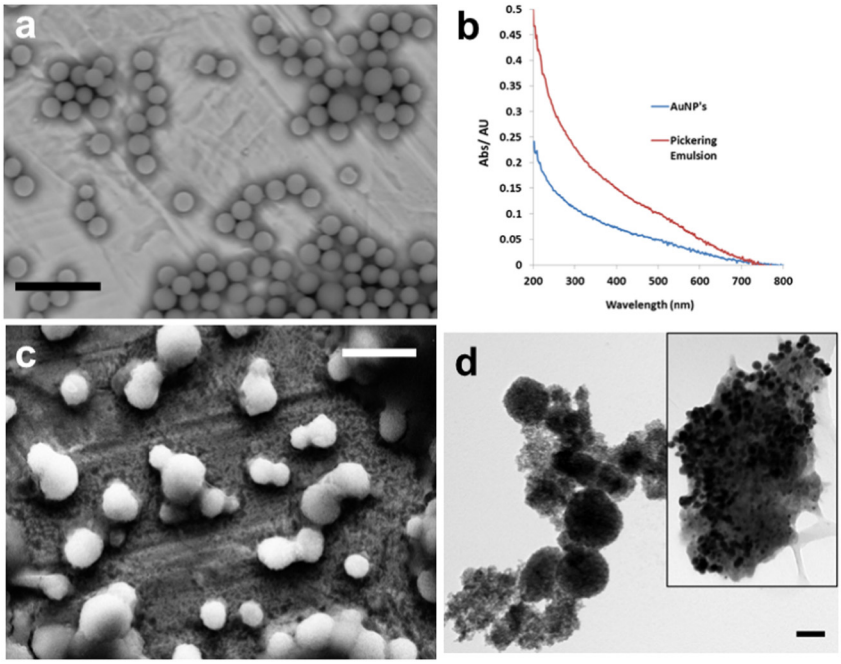

Fig. 2. a) Emulsion template 1.4 μm ± 0.05 Fe_3O_4 cores, create from emulsion droplets 11 μm ± 1, Fe_3O_4 at 3 mg/mL. Scale bar = 5 μm. b) Absorbance Spectra for 12-MDA stabilised AuNP's, and Pickering emulsions created from 12-MDA stabilised particles shown in panel c. c) Pickering Emulsions created from 12-MDA stabilised AuNP's, scale bar = 5 μm. d) TEM image of particles in part c, insert is a larger Au particle, scale bar for both = 100 nm.

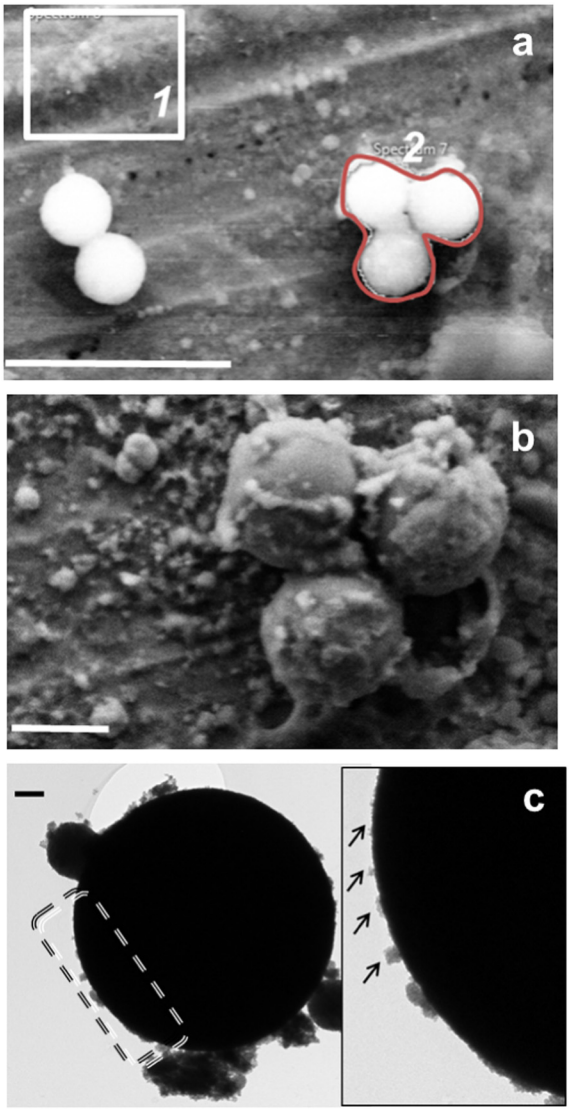

Fig. 3. a) SEM image of Fe_3O_4@Au particles, scale bar 5 μm. b) HRSEM image of Au@Fe_3O_4 particles, scale bar 1 μm. c) TEM image of Fe_3O_4 @Au particles, scale bar 200 nm, insert - magnified section shown in a check box of the microparticle surface.

emulsion shell. The SEM images of the particles are shown in Fig. 3a. The flow ratios for the fluids created emulsion droplets 8.8 μm ± 0.9 in size, and resultant particles were measured to be 1.5 μm ± 0.07 in size through analysis of the SEM images. This is comparable in size to the results obtained from experiment A1, suggesting the iron oxide core determines the eventual microparticle size. Some smaller particles were also observed under the SEM as shown in Fig. 3a - white box labelled 1, elemental analysis of the stub and particles, labelled 1 and 2 respectively in Fig. 3a are given in supplementary Fig. s3. A clear Au signal was observed on the microparticles (area 2), whereas only Cu signal (SEM stub material) was observed in area 1. It may be that these smaller particles are a cluster of AuNPs and that their signal is swamped by the Cu making it difficult to detect. Upon closer inspection using high resolution FEG-SEM, the surface of the microparticles appears rough as shown in Fig. 3b and suggests that the Au shell phase separates or forms clumps on the surface of the particle further analysis via TEM confirms this as shown in Fig. 3c. The TEM image (Fig. 3c insert) does appear to show a layer of Au particles across the surface of the Fe_3O_4 microparticles.

It was then possible to produce Fe_3O_4@Au particles via the Pickering emulsion, however the resultant microparticles may not have a uniform coating of AuNPs on their surface.

Here we present a method for the rapid assembly of nanomaterials at the liq-liq interface of an emulsion droplet. By placing the nanomaterials either outside/inside on both sides of the emulsion droplet, a shell/core or core@shell particle can be produced. In the absence of a core (inner particle), the AuNP shell was found to be unstable under the TEM beam, but appeared to form stable, micron sized particles when viewed under the SEM. Further studies are needed to show the stability of the shells under any external force, which may limit their applications, but the facile nature of the process opens up rapid and cost effective methods of materials synthesis. This we believe is the first demonstration of Pickering emulsions within a microfluidics chip for the production of Fe_3O_4@Au particles. The technique has the advantages of not requiring long reaction times, surfactants or templates to produce the asymmetric materials.

Acknowledgements

The work was supported by the European Commission for Research (PCIG11-GA-2012-321836 Nano4Bio).

Appendix A. Supplementary data

Supplementary data to this article can be found online at http://dx.doi.org/10.1016/j.colcom.2016.12.005.

References

[1] P.R. Sajanlal, T.S. Sreeprasad, A.K. Samal, T. Pradeep, Anisotropic nanomaterials: structure, growth, assembly, and functions, 2 (2011).
[2] M. Stratakis, H. Garcia, Catalysis by supported gold nanoparticles: beyond aerobic oxidative processes, Chem. Rev. 112 (2012) 4469–4506.
[3] M. Holzinger, A. Le Goff, S. Cosnier, Nanomaterials for biosensing applications: a review, Front. Chem. 2 (2014) 63.
[4] H. Liu, D. Chen, L. Li, T. Liu, L. Tan, X. Wu, F. Tang, Multifunctional gold nanoshells on silica nanorattles: a platform for the combination of photothermal therapy and chemotherapy with low systemic toxicity, Angew. Chem. Int. Ed. 50 (2011) 891–895.
[5] M. Tohidi, F.A. Mahyari, A.A. Safavi, Seed-less method for synthesis of ultra-thin gold nanosheets by using a deep eutectic solvent and gum Arabic and their electrocatalytic application, RSC Adv. 5 (2015) 32744–32754.
[6] R. Bardhan, S. Lal, A. Joshi, N.J. Halas, Theranostic nanoshells: from probe design to imaging and treatment of cancer, Acc. Chem. Res. 44 (2011) 936–946.
[7] C. Muehlethaler, M. Leona, J.R. Lombardi, Review of surface enhanced Raman scattering applications in forensic science, Anal. Chem. 88 (2016) 152–169.
[8] J.B. Edel, A.A. Kornyshev, A.R. Kucernak, M. Urbakh, Fundamentals and applications of self-assembled PLASMONIC nanoparticles at interfaces, Chem. Soc. Rev. 45 (2016) 1581–1596.
[9] R.A.W. Dryfe, Modifying the liquid/liquid interface: pores, particles and deposition, Phys. Chem. Chem. Phys. 8 (2006) 1869–1883.
[10] K. Banu, T. Shimura, Synthesis of large-scale transparent gold nanosheets sandwiched between stabilizers at a solid-liquid interface, New J. Chem. 36 (2012) 2112–2120.
[11] M. Platt, R.A.W. Dryfe, E.P.L. Roberts, Controlled deposition of nanoparticles at the liquid-liquid interface, Chem. Commun. (2002) 2324–2325.
[12] M. Platt, R.A.W. Dryfe, E.P.L. Roberts, Structural and electrochemical characterisation of Pt and Pd nanoparticles electrodeposited at the liquid/liquid interface, Electrochim. Acta 49 (2004) 3937–3945.
[13] C.N.R. Rao, K.P. Kalyanikutty, The liquid–liquid interface as a medium to generate nanocrystalline films of inorganic materials, Acc. Chem. Res. 41 (2008) 489–499.
[14] W. Ramsden, Separation of solids in the surface-layers of solutions and "suspensions" (observations on surface-membranes, bubbles, emulsions, and mechanical coagulation). – preliminary account, Proc. R. Soc. Lond. 72 (1903) 156–164.
[15] S.U. Pickering, CXCVI.-Emulsions, J. Chem. Soc. Trans. 91 (1907) 2001–2021.
[16] T. Wu, H. Wang, B. Jing, F. Liu, P.C. Burns, C. Na, Multi-body coalescence in Pickering emulsions, Nat. Commun. 6 (2015).
[17] S. Fouilloux, F. Malloggi, J. Daillant, A. Thill, Aging mechanism in model Pickering emulsion, Soft Matter 12 (2016) 900–904.
[18] S. Sihler, A. Schrade, Z. Cao, U. Ziener, Inverse Pickering emulsions with droplet sizes below 500 Nm, Langmuir 31 (2015) 10392–10401.
[19] Z. Nie, J.I. Park, W. Li, S.A.F. Bon, E. Kumacheva, An "inside-out" microfluidic approach to monodisperse emulsions stabilized by solid particles, J. Am. Chem. Soc. 130 (2008) 16508–16509.
[20] Y. Zhao, Z. Chen, X. Zhu, M.A. Möller, Facile one-step approach toward polymer@SiO_2 core–shell nanoparticles via a surfactant-free miniemulsion polymerization technique, Macromolecules 49 (2016) 1552–1562.
[21] S. Laurent, M. Mahmoudi, Superparamagnetic iron oxide nanoparticles: promises for diagnosis and treatment of cancer, Int. J. Mol. Epidemiol. Genet. 2 (2011) 367–390.

[22] M. Brust, M. Walker, D. Bethell, D.J. Schiffrin, R. Whyman, Synthesis of thiol-derivatised gold nanoparticles in a two-phase Liquid–Liquid system, 2000 801–802.
[23] H. Shang, W.-S. Chang, Kan, S.A. Majetich, G.U. Lee, Synthesis and characterization of paramagnetic microparticles through emulsion-templated free radical polymerization, Langmuir 22 (2006) 2516–2522.
[24] J.J. O'Mahony, M. Platt, D. Kilinc, G. Lee, Synthesis of superparamagnetic particles with tunable morphologies: the role of nanoparticle–nanoparticle interactions, Langmuir 29 (2013) 2546–2553.
[25] K. Yamanaka, S. Nishino, K. Naoe, M. Imai, Preparation of highly uniform Pickering emulsions by mercaptocarboxylated gold nanoparticles, Colloids Surf. A Physicochem. Eng. Asp. 436 (2013) 18–25.